

## RESEARCH ARTICLE

# Mitochondrial biogenesis is required for axonal growth

Annika Vaarmann, Merle Mandel, Akbar Zeb, Przemyslaw Wareski, Joanna Liiv, Malle Kuum, Eva Antsov, Mailis Liiv, Michal Cagalinec, Vinay Choubey and Allen Kaasik\*

## ABSTRACT

During early development, neurons undergo complex morphological rearrangements to assemble into neuronal circuits and propagate signals. Rapid growth requires a large quantity of building materials, efficient intracellular transport and also a considerable amount of energy. To produce this energy, the neuron should first generate new mitochondria because the pre-existing mitochondria are unlikely to provide a sufficient acceleration in ATP production. Here, we demonstrate that mitochondrial biogenesis and ATP production are required for axonal growth and neuronal development in cultured rat cortical neurons. We also demonstrate that growth signals activating the CaMKK $\beta$ , LKB1-STRAD or TAK1 pathways also co-activate the AMPK–PGC-1 $\alpha$ –NRF1 axis leading to the generation of new mitochondria to ensure energy for upcoming growth. In conclusion, our results suggest that neurons are capable of signalling for upcoming energy requirements. Earlier activation of mitochondrial biogenesis through these pathways will accelerate the generation of new mitochondria, thereby ensuring energy-producing capability for when other factors for axonal growth are synthesized.

**KEY WORDS:** Mitochondrial biogenesis, Neuronal growth, PGC-1 $\alpha$ , PPARGC1A

## INTRODUCTION

During early development, neurons undergo complex morphological rearrangements to assemble into neuronal circuits and propagate signals. Immature neurons start as round neuronal spheres, then gradual neurite outgrowth and elongation is followed by axon differentiation, dendritic arborisation and synapse formation. Rapid growth requires a large quantity of building material and efficient intracellular transport (Chada and Hollenbeck, 2003; Morris and Hollenbeck, 1993; Prokop, 2013; Sheng, 2014). It can be assumed that neuronal growth also requires a considerable amount of energy, both for the synthesis of raw material and for the delivery of this material to distal axonal locations. Although ATP can readily diffuse through the cytosol, it appears that the precise location of mitochondria is important during axogenesis and synaptogenesis in order to respond adequately to rapidly changing regional metabolic requirements. Previous studies have shown that depletion of mitochondria at or before axogenesis prevents axon formation (Mattson and Partin, 1999). Similarly, a lack of synaptic or terminal axonal mitochondria results in aberrant organelle transport and dysfunctional synapses. Furthermore,

addition of ATP partially rescues these defects (Lee and Peng, 2008; Verstreken et al., 2005). Thus, it seems that the local energy capacity at the active growth site is critical.

One may hypothesize that to produce this immediate/rapid energy, the neuron cannot rely entirely on pre-existing mitochondria, which are unlikely to provide a sufficient acceleration in ATP production. Thus, a neuron in active growth status should be capable of inducing mitochondrial biogenesis. The cellular energy status is monitored by AMP-activated protein kinase (AMPK), which senses the increase in cytosolic AMP and ADP levels that occurs when energy consumption exceeds energy production (Kahn et al., 2005; Zong et al., 2002). Activated AMPK phosphorylates the mitochondrial master regulator peroxisome proliferator-activated receptor gamma coactivator-1 $\alpha$  (PGC-1 $\alpha$ ; also known as PPARGC1A) (Jäger et al., 2007). Phosphorylated PGC-1 $\alpha$  then activates the nuclear respiratory factors NRF1 and NRF2, which in turn regulate the expression of both mitochondrial and nuclear genes encoding respiratory chain subunits and other proteins that are required for mitochondrial function (Wu et al., 1999). This process, however, will take hours if not days, and during this period the energy deficit might suppress or even block energy-consuming activities, such as neuronal growth. Thus, neurons should be capable of activating mitochondrial biogenesis machinery based not only on an energy deficit but also to pre-emptively sense upcoming energy requirements. Indeed, AMPK may also be activated by different kinases including the tumour-suppressor protein kinase LKB1 (also known as STK11) (Sakamoto et al., 2005; Woods et al., 2003), calcium/calmodulin-dependent protein kinase kinase (CaMKK $\beta$ ; also known as CAMKK2) (Hawley et al., 1995; Woods et al., 2005) and transforming growth factor- $\beta$ -activated kinase 1 (TAK1; also known as MAP3K7) (Momcilovic et al., 2006; Xie et al., 2006), which could potentially sense a wider range of signals in neurons than AMPK itself and thereby signal not only an energy deficit to PGC-1 $\alpha$  but also an upcoming energy need.

Our aim was to examine whether neuronal growth depends on mitochondrial biogenesis and whether the activation of cell growth pathways also promotes mitochondrial biogenesis to support the energetic needs of neuronal development. We demonstrate that several pathways activating neuronal growth also co-activate mitochondrial biogenesis through the AMPK–PGC-1 $\alpha$ –NRF1 axis to ensure energy for upcoming growth. We also demonstrate that mitochondrial biogenesis and local ATP production are required for axonal growth and neuronal development.


## RESULTS

### Activation of mitochondrial biogenesis increases axonal growth and neuronal development

We first performed a time-lapse experiment in which we followed axonal growth in control or PGC-1 $\alpha$ -overexpressing cultured rat neurons plated in separated compartments of the same dish (Fig. 1A,B). This set-up allowed us to visualise axonal growth

Department of Pharmacology, Centre of Excellence for Translational Medicine, Institute of Biomedicine and Translational Medicine, University of Tartu, Ravila 19, Tartu 51014, Estonia.

\*Author for correspondence (allen.kaasik@ut.ee)

 A.K., 0000-0002-4850-3198

Received 23 July 2015; Accepted 7 April 2016

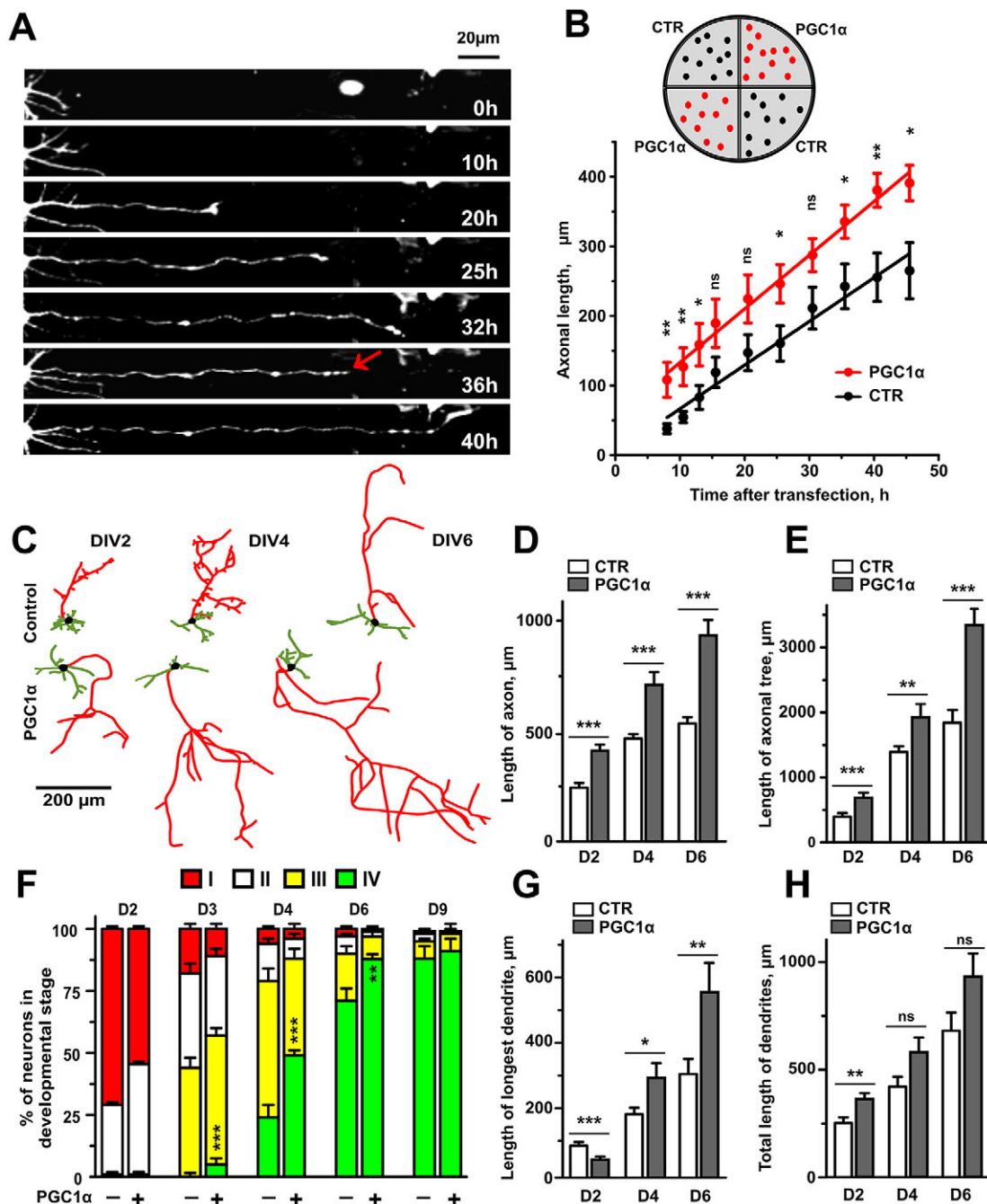


**Fig. 1. PGC-1 $\alpha$  enhances neuronal development and maturation in cultured rat cortical neurons.** Primary cortical neurons were transfected with GFP- and PGC-1 $\alpha$ -overexpressing plasmids at DIV (day *in vitro*) 1, and neuronal outgrowth was followed for 48 h by confocal microscopy using a live cell imaging chamber. (A) Time-lapse confocal images of individual neurons in culture showing axonal growth at different time points after transfection. The arrow indicates spontaneous axonal retraction during initial axonal elongation. (B) The growth of axons in different groups was followed simultaneously from compartmentalised cell culture dishes (illustrated above). The speed of axonal elongation was significantly higher in PGC-1 $\alpha$ -overexpressing neurons (slope  $7.71 \pm 0.28$ ) when compared with the control group (CTR; slope  $6.28 \pm 0.42$ ;  $n=20$  axons,  $P=0.012$ ). (C) Neurolucida reconstructions of control (above) and PGC-1 $\alpha$ -overexpressing (below) neurons at different days *in vitro*. Green, dendrites; red, axons. (D,E) Quantification of axonal morphology shows that overexpression of PGC-1 $\alpha$  results in longer axonal roots (D) and total lengths of the axonal tree (E) at DIV2 to DIV6 ( $n=30$  axons). (F) Results from analysis of neuronal morphology at different culture days ( $n \geq 90$  fields). Maturation stages: I, round cells, formation of lamellipodia; II, immature neuron, sprouting of several minor neurites; III, axon and dendrite formation, neuronal polarisation and branching; IV, neuron with adult-like morphology, ongoing maturation of differentiated processes. (G,H) Quantification of longest dendrite (G) or total dendritic length (H) following PGC-1 $\alpha$  overexpression ( $n=30$ ). \* $P < 0.05$ , \*\* $P < 0.01$ , \*\*\* $P < 0.001$  compared with control groups; ns, not significant.

simultaneously and under similar conditions over 48 h in different groups. Statistical analysis of the growth of 20 axons from each group demonstrated that PGC-1 $\alpha$  overexpression accelerated axonal

elongation significantly (Fig. 1B). These changes were even more evident at later stages of development (24 to 120 h after transfection), when axonal length in PGC-1 $\alpha$ -overexpressing

neurons exceeded that of control neurons (Fig. 1C,D). Moreover, in addition to the main branch of the axon being longer in PGC-1 $\alpha$ -overexpressing neurons, the entire axonal tree was longer (Fig. 1E) and, in general, more mature (Fig. 1F). We performed a similar analysis of dendrites and the total length of dendrites per neuron, although these changes were less evident at later time points (Fig. 1G,H). Thus, PGC-1 $\alpha$  overexpression accelerates neuronal growth and maturation, suggesting that mitochondrial biogenesis, and presumably mitochondrion-derived energy, is a limiting factor for these processes.

In a second set of experiments, we tested whether reduced energy support or suppression of mitochondrial biogenesis would impair axonal outgrowth. Indeed, both inhibition of glycolysis by 2-deoxy-D-glucose (10 mM for 24 h) or oxidative phosphorylation by sodium azide (100  $\mu$ M for 24 h) suppressed axonal growth (Fig. S1). Suppression of mitochondrial biogenesis by PGC-1 $\alpha$ -specific shRNA decreased axonal growth slightly but significantly at DIV3 (from 423 $\pm$ 10  $\mu$ m in control to 393 $\pm$ 10  $\mu$ m in the shRNA-treated group,  $P=0.037$ ,  $n=188$ –190). The difference was more evident at DIV6 (from 971 $\pm$ 64  $\mu$ m in control to 781 $\pm$ 57  $\mu$ m in the shRNA-treated group,  $P=0.029$ ,  $n=37$ ). Similarly, suppression of the downstream target of PGC-1 $\alpha$ , NRF1 [which is known to activate mitochondrial biogenesis more specifically (Wu et al., 1999)], by expressing dominant-negative (dn) NRF1 suppressed axonal growth (from 386 $\pm$ 281  $\mu$ m in control to 307 $\pm$ 30  $\mu$ m in the dnNRF1 group,  $P=0.0006$ ,  $n=39$ ).

#### PGC-1 $\alpha$ increases mitochondrial density specifically in the peripheral axonal tree

We further characterised the spatial organisation of mitochondria in axons of control and PGC-1 $\alpha$ -overexpressing neurons. Indeed, as expected, PGC-1 $\alpha$  overexpression led to a very significant increase in the number and density of mitochondria in axons (Fig. 2A,B). However, this increase was not homogenous spatially, and there was a significant decrease in mitochondrial density towards the periphery (Fig. 2C). In further analysis that pooled data from ten control neurons, a clear negative relationship between distance from the soma and mitochondrial density was demonstrated (Fig. 2D; Spearman correlation  $P<0.0001$ ). Whereas close to the soma (<200  $\mu$ m from soma) the mitochondrial density exceeded 60%, it was less than 10% at the end of the axonal tree (>2000  $\mu$ m from soma). However, in PGC-1 $\alpha$ -overexpressing neurons, this density pattern was not so profound, and the density of mitochondria remained significantly higher at the end of the axonal tree (Fig. 2D,E). Indeed, further analysis demonstrated a clear positive relationship between the effect of PGC-1 $\alpha$  overexpression on mitochondrial abundance and distance from the body (Fig. 2F; Spearman correlation  $P<0.0001$ ). A decrease in mitochondrial density at the periphery in the control group was also associated with increased intervals between individual mitochondria; this distance was considerably smaller in PGC-1 $\alpha$ -overexpressing neurons (Fig. 2G;  $P<0.0001$ ). PGC-1 $\alpha$  overexpression also increased mitochondrial number and density in dendrites (Fig. 2H,I), where the most prominent effects were, similar to axons, distally (Fig. 2J). These results demonstrate that mitochondrial density is lowest at the end of the axonal tree (e.g. in areas of active growth) and that it is the mitochondrial density in neuronal endings that is most affected by activation of mitochondrial biogenesis.

To verify that the observed effects were associated with increased mitochondrial biogenesis and not with other potential effects of

PGC-1 $\alpha$  activation, we performed control experiments with NRF1. Similar to PGC-1 $\alpha$ , NRF1 overexpression increased mitochondrial density (Fig. 3A) and accelerated neuronal maturation (Fig. 3B). Co-expression of dnNRF1 suppressed the effect of PGC-1 $\alpha$  on mitochondrial biogenesis ( $P<0.05$ ), axonal growth ( $P<0.05$ ) and neuronal maturation ( $P<0.014$ ) (Fig. 3C–E;  $P$ -values for interaction between the two treatments, PGC-1 $\alpha$  and dnNRF1, two-way ANOVA).

We have previously demonstrated that PGC-1 $\alpha$  overexpression increases mitofusin 2 (*Mfn2*) promoter activity (Wareski et al., 2009). MFN2 is known to be directly regulated by PGC-1 $\alpha$ , independently of NRF2 (Wareski et al., 2009). To determine the functional outcome of increased MFN2, we quantified mitochondrial fusion events using the mitochondria-targeted photoconvertible KikGR1 protein. Overexpression of PGC-1 $\alpha$  led to a significant increase in fusion rate (Fig. S2A). No difference was observed in mitochondrial movement. The fraction of time spent moving and mitochondrial velocity remained similar between groups (Fig. S2B,C).

We also tested the effect of PGC-1 $\alpha$  shRNA on axonal mitochondrial density. The effect was variable between different sister cultures, causing a minimal to moderate negative effect on mitochondrial density. Nevertheless, a summary analysis pooling data from all independent experiments revealed a slight but significant decrease in axonal mitochondrial density (from 0.314 $\pm$ 0.005 in control to 0.296 $\pm$ 0.005 in the shRNA-treated group,  $P=0.013$ ,  $n=210$ –222 axons from five independent sister cultures). However, pooled data from experiments with dnNRF1 showed more stable inhibitory effects (from 0.343 $\pm$ 0.004 in control to 0.298 $\pm$ 0.003 in the dnNRF1-treated group,  $P<0.0001$ ,  $n=180$  axons from four independent sister cultures).

#### PGC-1 $\alpha$ increases the ATP/ADP ratio in axonal endings

Next, we estimated the cell ATP/ADP ratio using the genetically encoded fluorescent ratiometric probe PercevalHR, which senses ATP/ADP ratio (Tantama et al., 2013). Control experiments demonstrated either an increase in PercevalHR signal ( $F_{488nm}/F_{405nm}$ ) for individual axonal endings after reinfusion of glucose to glucose-deprived cells, or a decrease in signal after inhibition of mitochondrial ATP production by oligomycin, confirming the suitability of PercevalHR for tracking intracellular ATP/ADP levels in our model (Fig. 4A). This suggests that PercevalHR is sufficiently sensitive to detect an increase in axonal ATP levels under normal culture conditions. Further experiments performed at axonal endings of control and PGC-1 $\alpha$ -overexpressing neurons showed a statistically significant 23% increase in signal in the PGC-1 $\alpha$  group, suggesting an increase in ATP levels (Fig. 4B,C). The experiment was repeated twice with similar results.

These data are also supported by experiments in which we compared the relative ATP levels in control, PGC-1 $\alpha$ -overexpressing and PGC-1 $\alpha$  shRNA groups. Neurons were co-transfected with firefly and *Renilla* luciferase-expressing plasmids and the firefly luciferase activity was measured 72 h later in living cells using DMNPE-caged luciferin as a substrate. The results were normalised to *Renilla* luciferase activity measured after cell lysis. A 12% increase in ATP levels was observed in neurons overexpressing PGC-1 $\alpha$ , whereas a 25% decrease was observed when PGC-1 $\alpha$  was silenced (Fig. S3).

#### Activation of mitochondrial biogenesis is required for AMPK-induced neuronal growth

Our findings suggested that activation of PGC-1 $\alpha$  and mitochondrial biogenesis might be a limiting factor for neuronal



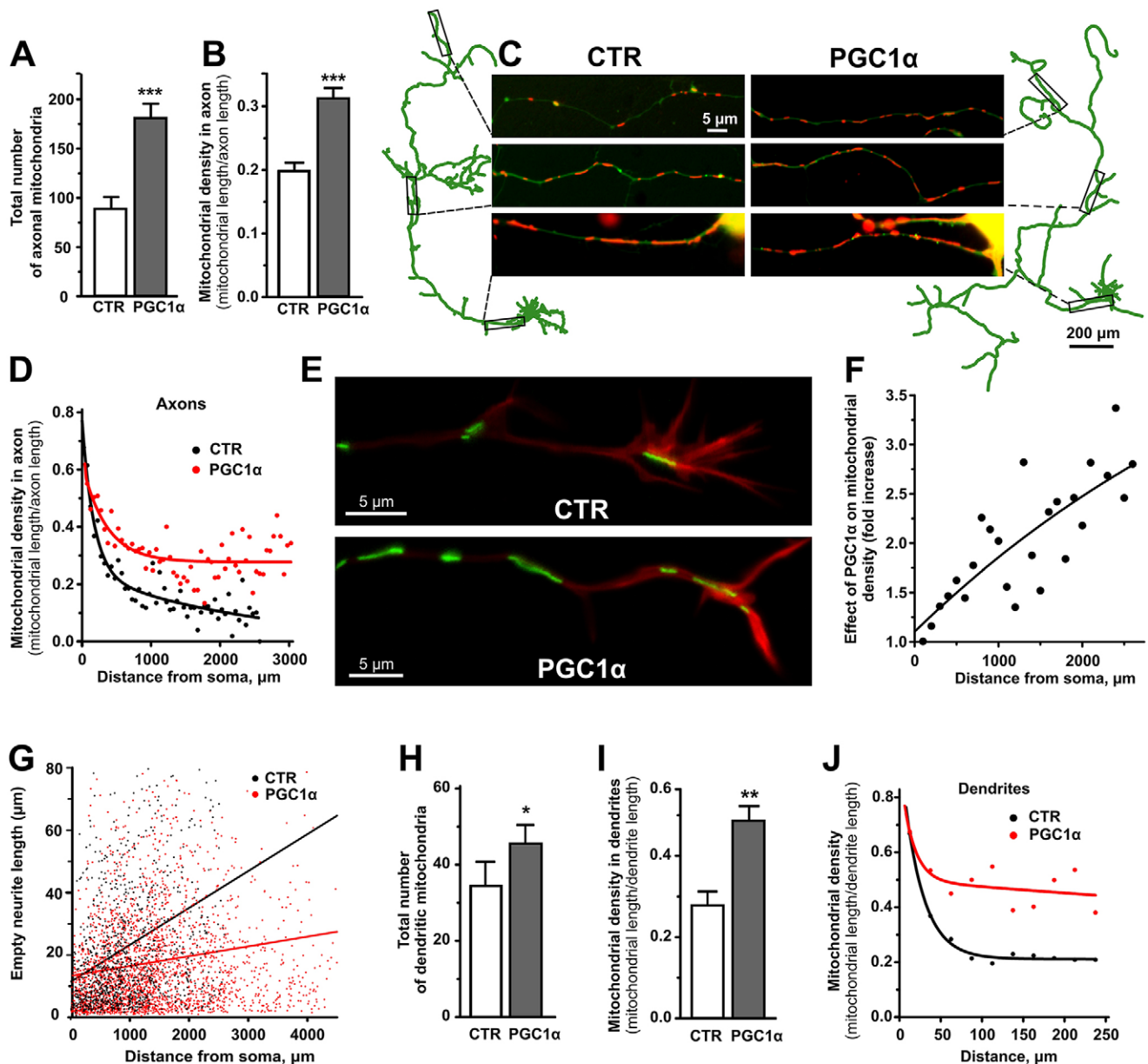


**Fig. 2. PGC-1 $\alpha$  regulates mitochondrial biogenesis and spatial organisation in developing neurons.** Primary cortical neurons were transfected with mito-DsRed, GFP and the plasmids of interest. (A,B) PGC-1 $\alpha$ -overexpressing neurons demonstrate increased axonal mitochondria (A) and a higher mitochondrial density (B) in axons at DIV6 ( $n=30$  neurons). (C) NeuroLucida reconstructions and fluorescence images of control (left) and PGC-1 $\alpha$ -overexpressing (right) neurons at DIV6. (D-G) Distribution of axonal mitochondria: mitochondrial density along the length of the axon (D) and representative images (E) depicting mitochondria (expressing mEos2-Mito) close to axonal growth cones (expressing Lifeact-mCherry). The effect of PGC-1 $\alpha$  overexpression on mitochondrial density increased along the length of the axon (F) and lengths unoccupied by mitochondria along axons decreased (G);  $n=10$  neurons. (H-J) Quantitative analysis of mitochondria in dendrites: total number (H) and average density (I) of dendritic mitochondria, and mitochondrial distribution along dendrites (J);  $n=10$  neurons. \* $P<0.05$ , \*\* $P<0.01$ , \*\*\* $P<0.001$  compared with respective control groups.

growth. We therefore aimed to identify upstream pathways that could link increased energy needs during neuronal development to enhanced mitochondrial biogenesis through activation of PGC-1 $\alpha$ . Activation of AMPK or its upstream kinase complex is known to activate PGC-1 $\alpha$  and neuronal growth (Roy Chowdhury et al., 2012; Shelly et al., 2007; Tao et al., 2014). In our settings, overexpression of constitutively active (ca) AMPK $\alpha$ 1 (also known as PRKAA1) and pharmacological activation of endogenous AMPK using 1.5 mM AICAR (or 0.5 mM metformin; Fig. S4) in cortical neurons increased transcriptional activity of PGC-1 $\alpha$  in a luminescence-based reporter assay (Fig. 5A), increased the

expression of mitochondrial genes (Fig. 5B), axonal growth (Fig. 5C;  $P<0.0199$  for interaction) and increased mitochondrial density in axons (Fig. 5D,E). Notably, the effect of caAMPK was completely abolished when PGC-1 $\alpha$  was suppressed by specific shRNA co-expression suggesting that its positive effect on mitochondrial biogenesis is mediated fully by PGC-1 $\alpha$  ( $P<0.0001$  for interaction). Moreover, activation of AMPK by overexpressing caAMPK accelerated neuronal maturation in a PGC-1 $\alpha$ -dependent manner (Fig. 5F;  $P<0.05$  for interaction). Inhibition of AMPK activity by overexpressing dnAMPK reduced both mitochondrial density (from  $0.370\pm0.009$  in control to  $0.324\pm0.010$  in the

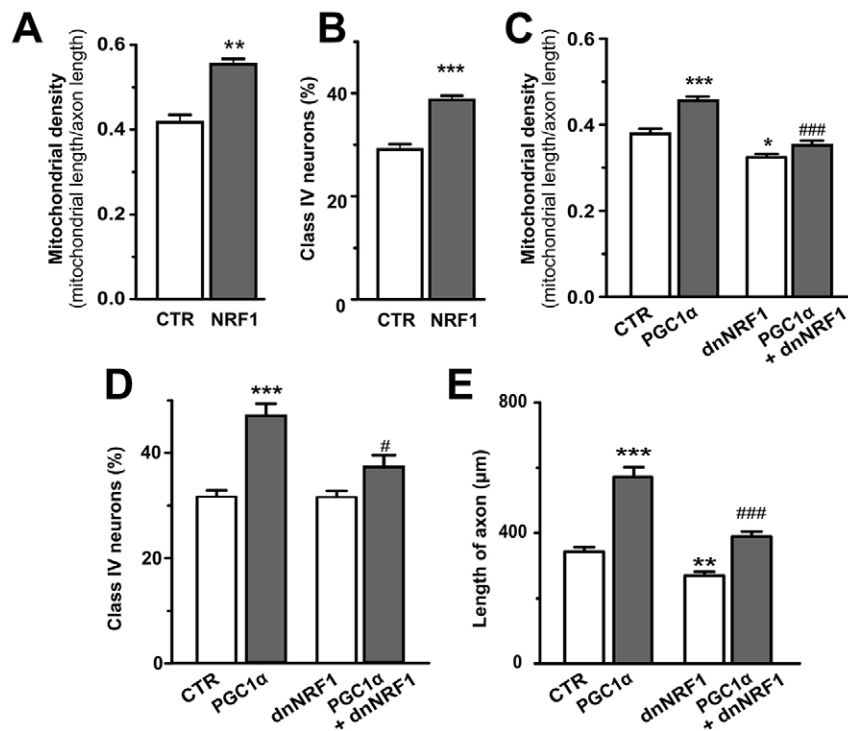


**Fig. 3. Effects of PGC-1α are mediated by the downstream regulator of mitochondrial biogenesis NRF1.** (A,B) Cortical neurons overexpressing NRF1 show higher mitochondrial density (A) and enhanced neuronal maturation (B). (C-E) Co-expression of dnNRF1 suppresses the effect of PGC-1α on mitochondrial biogenesis (C), neuronal maturation (D) and axonal length (E). \* $P < 0.05$ , \*\* $P < 0.01$ , \*\*\* $P < 0.001$  compared with the control group; # $P < 0.05$ , ### $P < 0.001$  compared with the PGC-1α group.  $n \geq 40$  axons for mitochondrial density and axonal growth,  $n = 120$  fields for neuronal maturation.

dnAMPK group,  $P = 0.001$ ,  $n = 109$ – $112$  axons from two independent sister cultures) and axonal outgrowth (from  $347 \pm 16$  in control to  $303 \pm 12$  in the dnAMPK group,  $P = 0.025$ ,  $n = 80$  axons from two independent sister cultures).

The energy-sensing capability of AMPK is known to also rely partly on its upstream kinase complex comprising STE-related adaptor (STRAD), mouse protein 25 (MO25; also known as CAB39) and LKB1 (a serine/threonine kinase), which is known to activate AMPK and thus possibly also PGC-1α. Indeed, PGC-1α transcriptional activity was increased when proteins belonging to this complex were overexpressed (Fig. 5G). Most prominently, overexpression of STRADα increased PGC-1α transcriptional activity almost fourfold and also activated PGC-1α-dependent mitochondrial density (Fig. 5I;  $P < 0.017$  for interaction). Importantly, STRADα also promoted axonal growth and neuronal development (Fig. 5H,J,K), but not when endogenous PGC-1α was

suppressed by shRNA (Fig. 5J,K;  $P < 0.026$  and  $P < 0.039$ , respectively, for interaction). Thus, activation of AMPK, either by overexpression or activation of its upstream kinase complex, cannot stimulate neuronal growth without co-activation of the PGC-1α pathway.

#### Co-activation of mitochondrial biogenesis is a prerequisite for CaMKKβ-induced neuronal growth

CaMKKβ, which is known to be a mediator of  $Ca^{2+}$  signals for neuronal growth, also phosphorylates AMPK (Woods et al., 2005). We attempted to test whether CaMKKβ activates endogenous PGC-1α to the extent required to activate mitochondrial biogenesis. Indeed, overexpression of CaMKKβ increased the transcriptional activity of PGC-1α twofold compared with control neurons (Fig. 6A), and it also caused a significant increase in mitochondrial density (Fig. 6B,C). This effect of CaMKKβ was

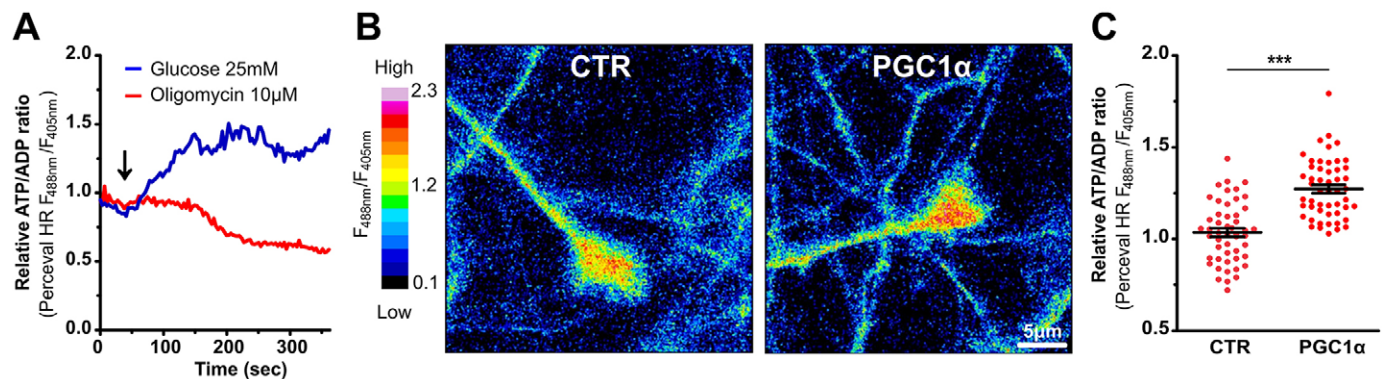


**Fig. 4. PGC-1α-induced mitochondrial biogenesis increases the ATP/ADP ratio in axonal endings.** (A) Cortical neurons transfected with the ATP/ADP sensor PercevalHR were treated with glucose (25 mM) after glucose deprivation or oligomycin (10 μM, both used as positive controls), showing either an increase or decrease in the PercevalHR ratiometric signal ( $F_{488nm}/F_{405nm}$ ) in axonal endings. (B) Pseudocolour ratiometric images of an axonal ending of control and PGC-1α-overexpressing neurons expressing PercevalHR. (C) Quantification of ATP/ADP ratios in the axonal endings of control and PGC-1α-overexpressing neurons ( $n = 50$  neurons per group). \*\*\* $P < 0.001$  compared with the control group.

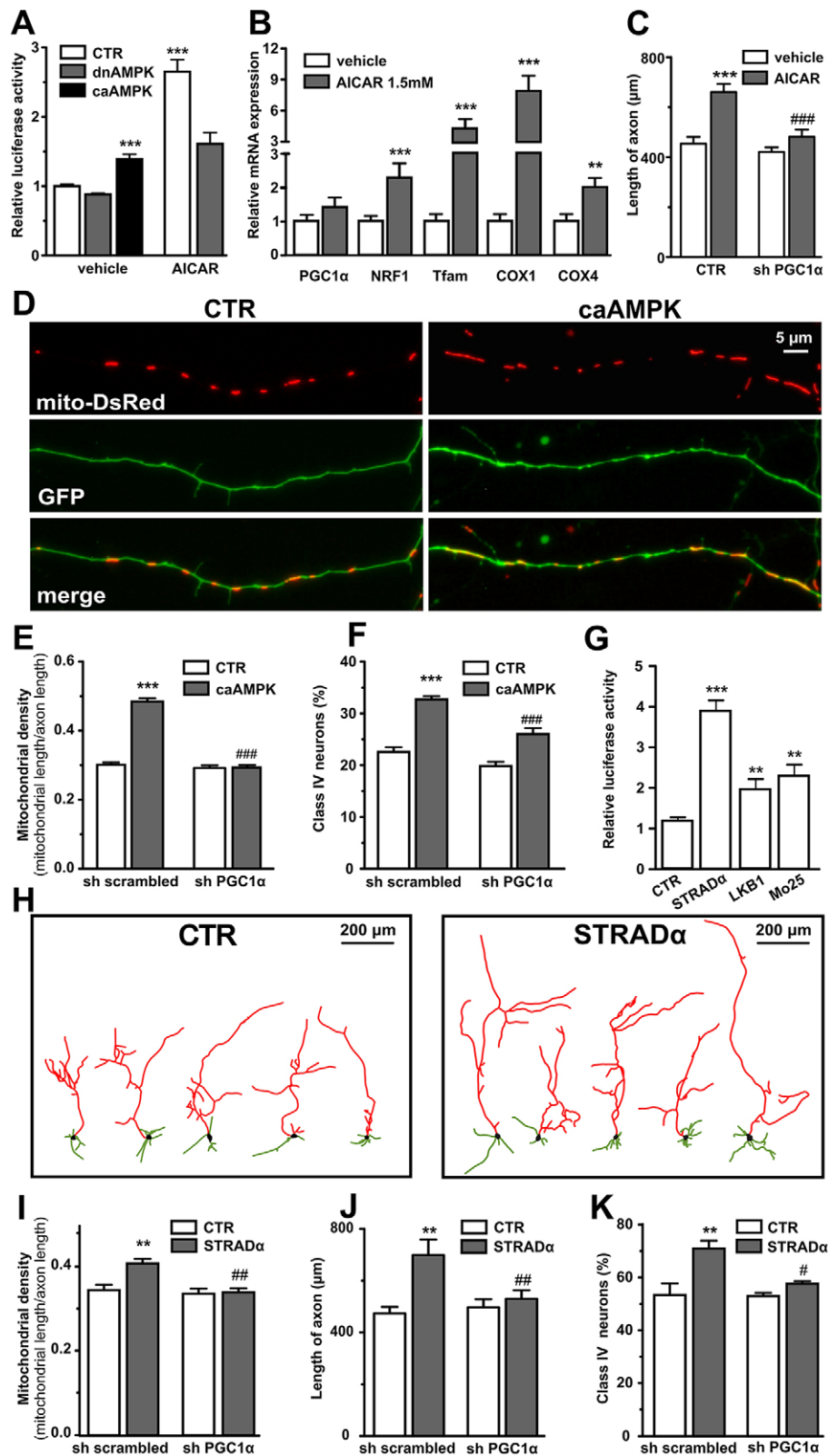


**Fig. 5. AMPK and its upstream kinase complex regulate PGC-1α-dependent mitochondrial biogenesis and neuronal growth.** (A) A luciferase reporter assay shows that active AMPK increases transcriptional activity of GAL4-PGC-1α in cortical neurons and that AICAR (1.5 mM, 24 h) modulates PGC-1α transcriptional activity by activating AMPK. The firefly luciferase signal is normalised to *Renilla* luciferase. (B) Quantitative PCR analysis of mitochondrial biogenesis and energy production-related genes in primary cortical neurons following AICAR treatment. The mRNA levels of *PGC-1α* (*Ppargc1a*), *Nrf1*, *Tfam*, *Cox1* and *Cox4* (cytochrome c oxidase subunits 1 and 4, which are encoded in mitochondrial and nuclear DNA, respectively) were normalised to *Hprt* mRNA levels and expressed relative to control groups ( $n=4$  dishes). (C) Treatment of cortical neurons with the AMPK activator AICAR promotes axonal growth in a PGC-1α-dependent manner. (D) Examples of cortical neurons expressing mito-DsRed, GFP and caAMPK. Images depict mitochondrial distribution in the distal part of axons. (E,F) Overexpression of caAMPK in cortical neurons increases mitochondrial density in axons significantly (E) and enhances neuronal maturation (F). These effects are diminished by overexpression of PGC-1α shRNA. \*\* $P<0.01$ , \*\*\* $P<0.001$  compared with the control group; ### $P<0.001$  compared with the caAMPK group. (G) Components of the AMPK upstream kinase complex show varying impacts on PGC-1α transcriptional activity in luciferase assays. (H) Neurolucida reconstructions of control and STRADα-overexpressing primary neurons at DIV6. (I-K) Quantitation of mitochondrial density in axons (I), axonal length (J) and neuronal maturation (K) after overexpression of STRADα or PGC-1α shRNA. \*\* $P<0.01$  compared with control group; # $P<0.05$ , ## $P<0.01$  compared with the STRADα group.  $n\geq 8$  wells for luciferase activity,  $n\geq 40$  axons for density and axonal growth,  $n=120$  fields for neuronal maturation.

clearly mediated by the AMPK–PGC-1α–NRF1 pathway because co-expression of dnAMPK ( $P<0.0002$ ), a PGC-1α shRNA-encoding plasmid ( $P<0.0001$ ) or dnNRF1 ( $P<0.0002$ ) abolished the effect of CaMKKβ on mitochondrial density (Fig. 6C–E;  $P$ -values for interaction).

Overexpression of CaMKKβ also increased axonal growth and the number of stage IV neurons at DIV4 (Fig. 6F–H). Importantly, the effects of CaMKKβ required activation of the AMPK–PGC-1α–NRF1 pathway because co-expression of dnAMPK, PGC-1α shRNA or dnNRF1 abolished the effects of CaMKKβ (Fig. 6G–K).



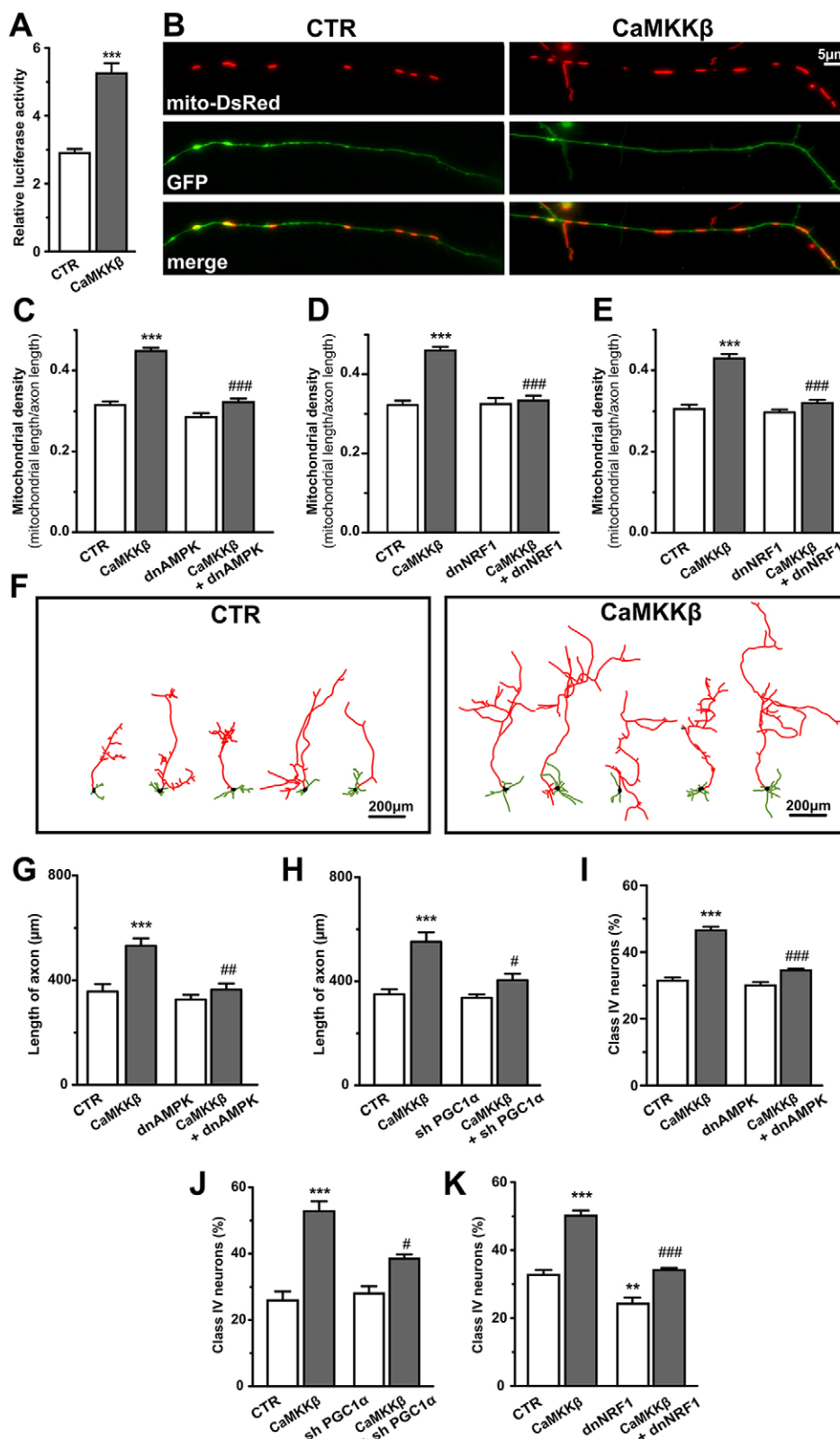


**Fig. 6. Activation of PGC-1 $\alpha$  is required for CaMKK $\beta$ -induced mitochondrial biogenesis and neuronal growth.** (A) A luciferase reporter assay shows increased transcriptional activity of GAL4-PGC-1 $\alpha$  in CaMKK $\beta$ -overexpressing neurons ( $n \geq 8$  wells). (B) Representative images of cortical neurons at DIV6, demonstrating mito-DsRed and GFP signal following CaMKK $\beta$  overexpression. (C–E) CaMKK $\beta$  activates mitochondrial biogenesis; however, this effect is abolished when dnAMPK (C), PGC-1 $\alpha$  shRNA (D) or dnNRF1 (E) is co-expressed in primary neurons. \*\*\* $P < 0.001$  compared with the control group; ### $P < 0.001$  compared with the CaMKK $\beta$  group. (F) Representative images of control or CaMKK $\beta$ -expressing neurons at DIV6. (G–K) Morphological analysis of neurons demonstrates the impact of CaMKK $\beta$  on neuronal axonal elongation (G,H) and maturation (I–K). The positive effects of CaMKK $\beta$  are abolished when co-expressed with dnAMPK (G,I;  $P < 0.02$  and  $P < 0.0001$ , respectively, for interaction, two-way ANOVA), PGC-1 $\alpha$  shRNA (H,J;  $P < 0.026$  and  $P < 0.005$ , respectively, for interaction) or dnNRF1 (K;  $P < 0.022$  for interaction). \*\* $P < 0.01$ , \*\*\* $P < 0.001$  compared with control group; # $P < 0.05$ , ## $P < 0.01$ , ### $P < 0.001$  compared with the CaMKK $\beta$  group.  $n \geq 40$  axons for density and axonal growth,  $n = 120$  fields for neuronal maturation.

### Co-activation of mitochondrial biogenesis is also a prerequisite for TGF $\beta$ -TAK1-induced neuronal growth

TAK1, activated by TGF $\beta$  signalling, controls axonal growth during brain development (Yi et al., 2010). However, it has also been shown that TAK1 activates AMPK (Xie et al., 2006). We therefore

asked whether activation of the TGF $\beta$ -TAK1 pathway can co-activate PGC-1 $\alpha$ -dependent mitochondrial biogenesis. Indeed, overexpression of TAK1 increased transcriptional activity of PGC-1 $\alpha$  (Fig. 7A) and mitochondrial density (Fig. 7B). The latter was not visible when endogenous AMPK was suppressed by

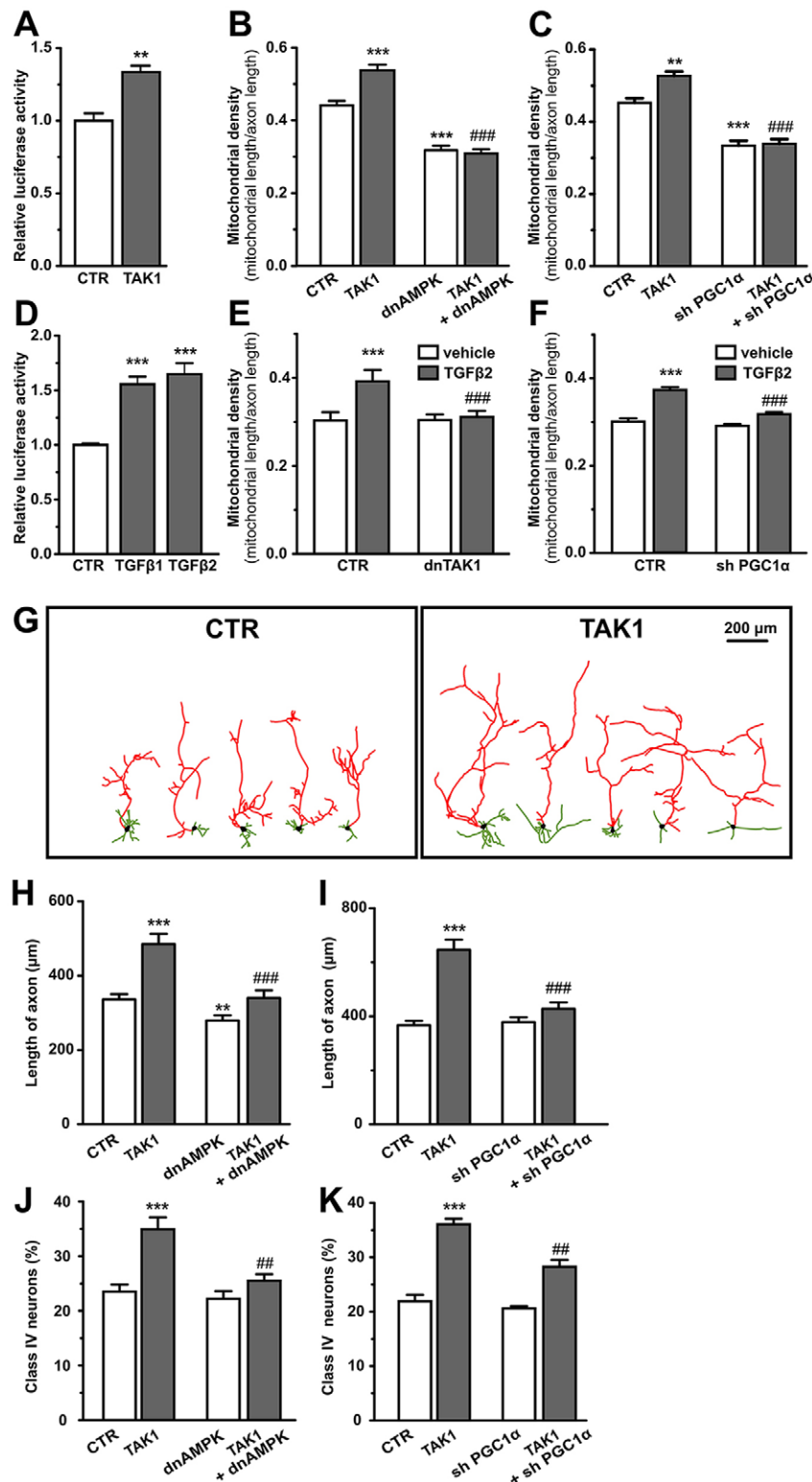


**Fig. 7. TAK1 and TGFβ regulate mitochondrial biogenesis and neuronal maturation via PGC-1α.** (A) A luciferase reporter assay shows increased transcriptional activity of GAL4-PGC-1α in TAK1-overexpressing neurons ( $n \geq 8$  wells). (B,C) TAK1 enhances PGC-1α-dependent (B) and AMPK-dependent (C) mitochondrial density in neurons. \*\* $P < 0.01$ , \*\*\* $P < 0.001$  compared with the control; ### $P < 0.001$  compared with the TAK1 group. (D) Both TGFβ1 and TGFβ2 increase PGC-1α transcriptional activity. (E,F) The effect of TGFβ2 on mitochondrial biogenesis is TAK1 (E) and PGC-1α (F) dependent. \*\*\* $P < 0.001$  compared with the control; ### $P < 0.001$  compared with the TGFβ2 group. (G) NeuroLucida reconstructions of control and TAK1-overexpressing neurons at DIV6. (H-K) Results of neuronal morphology analysis following co-expression of TAK1 and PGC-1α shRNA or dnAMPK. \*\* $P < 0.01$ , \*\*\* $P < 0.001$  compared with control group; ## $P < 0.01$ , ### $P < 0.001$  compared with the TAK1 group.  $n \geq 8$  wells for luciferase activity,  $n \geq 40$  axons for density and axonal growth,  $n = 120$  fields for neuronal maturation.

dnAMPK (Fig. 7B;  $P < 0.0001$  for interaction) or endogenous PGC-1α by specific shRNA (Fig. 7C;  $P < 0.0078$  for interaction).

PGC-1α transcriptional activity and mitochondrial density were similarly increased when we treated neurons with TGFβ1 or TGFβ2 (72 h, 50 ng/ml; Fig. 7D,E). This effect was mediated by the TAK1–PGC-1α pathway because co-expression of dominant negative (dn) TAK1 ( $P < 0.04$ ) or a PGC-1α shRNA-encoding plasmid ( $P < 0.002$ )

abolished the effect of TGFβ2 on mitochondrial biogenesis (Fig. 7E,F;  $P$ -values for interaction).

TAK1 overexpression also accelerated axonal growth (Fig. 7G-I) and maturation (Fig. 7J,K). These effects required activation of the AMPK–PGC-1α pathway because co-expression of dnAMPK (Fig. 7H,J;  $P < 0.04$  and  $P < 0.03$ , respectively, for interaction) or PGC-1α shRNA (Fig. 7I,K;  $P < 0.0006$  and  $P < 0.015$ , respectively,



for interaction) suppressed the effect of TAK1 overexpression on axonal growth and maturation. Similarly, TGF $\beta$ 2 enhanced neuronal maturation (the percentage of stage IV neurons increased from  $29.7 \pm 0.6$  to  $36.4 \pm 1.1$ ;  $P=0.002$ ), an effect that was abolished by dnAMPK ( $P<0.046$  for interaction).

## DISCUSSION

### Mitochondrial biogenesis is required for neuronal growth

One of the most striking findings of this study is that mitochondrial biogenesis itself is required for axonal growth. We have previously demonstrated that PGC-1 $\alpha$  and PGC-1 $\beta$  (PPARGC1B) levels and activity control mitochondrial number and energy production both in axons and the cell body (Wareski et al., 2009). Recent findings indicate that PGC-1 $\alpha$  also controls mitochondrial density in dendrites (Cheng et al., 2012).

Here, we demonstrate that PGC-1 $\alpha$  overexpression leads to an average twofold increase in the total number of mitochondria in the axonal tree. This increase, however, is not homogenous between compartments: close to the cell body, PGC-1 $\alpha$  causes less of an increase in mitochondrial density, but increases it almost threefold at the end of the axonal tree. Of note, PGC-1 $\alpha$  also increases the ATP/ADP ratio in axonal endings. Increased mitochondrial density specifically in the periphery of PGC-1 $\alpha$ -overexpressing neurons cannot be explained by simple redistribution of mitochondria from the cell body to the periphery because PGC-1 $\alpha$  overexpression does not decrease mitochondrial density in the neuronal body (Wareski et al., 2009). Instead, this could be explained by an increased mitochondrial fusion rate helping to distribute mitochondria more homogeneously throughout the PGC-1 $\alpha$ -overexpressing cell.

These changes were accompanied by an acceleration in axonal growth and neuronal development. dnNRF1 suppressed the effects of PGC-1 $\alpha$  on both mitochondrial biogenesis and neuronal growth, demonstrating that activation of mitochondrial biogenesis directly activates neuronal growth. Interestingly, neurons overexpressing PGC-1 $\alpha$  exhibited a significant increase in mitochondrial density in dendrites, which is consistent with a previous report (Cheng et al., 2012); however, we observed only a slight increase in the total number of dendritic mitochondria and a modest change in dendritic length. Hence, these findings emphasize the need to generate new mitochondria to support neuronal growth. Our results imply that mitochondrial biogenesis, or rather mitochondrial mass and local ATP production, is itself a limiting factor for axonal growth. Indirectly, these results prompt the speculation that axons develop, at least *in vitro*, under conditions of chronic energy deficit.

### Do neurons have a mechanism to sense upcoming energy needs?

To meet the increased energy needs associated with neuronal development, neurons require machinery and mechanisms that sense energy requirements and increase their energy production capacity. It has been proposed that a persistent energy deficit will lead to activation of AMPK, which in turn activates mitochondrial biogenesis to produce new mitochondria that will begin to produce additional energy. This process, however, could take a considerable amount of time, during which the neuron has to develop and survive under conditions of energy deficit.

However, here we suggest that growth signals could co-activate the AMPK–PGC-1 $\alpha$ –NRF1 axis before the energy deficit. Neuronal activity (for example) that involves an increase in cytosolic calcium will also lead to activation of CaMKK $\beta$  (Hudmon and Schulman, 2002). Activation of CaMKK $\beta$  in turn increases AMPK activity, thereby increasing the transcriptional activity of PGC-1 $\alpha$  and

promoting mitochondrial biogenesis. It has recently been demonstrated that an increase in cAMP levels leads to activation of LKB1, which then activates AMPK. The role of cAMP in axon initiation during neuronal polarisation is to regulate the downstream kinase LKB1 by phosphorylation (Barnes et al., 2007; Shelly et al., 2007), which also co-activates mitochondrial biogenesis through AMPK. Furthermore, TAK1, which is activated by TGF $\beta$  signalling and controls axonal growth, co-activates mitochondrial biogenesis through AMPK (White et al., 2008; Xie et al., 2006; Yu et al., 2014). Our data suggest that these AMPK upstream kinases cannot stimulate neuronal growth without co-activation of the PGC-1 $\alpha$  pathway. PGC-1 $\alpha$  shRNA suppressed most of the axonal growth induced by STRAD $\alpha$ , CAMKK $\beta$  and TAK1. There were also strong interactions statistically between STRAD $\alpha$ , CAMKK $\beta$  and TAK1 alone compared with these treatments when they were combined with PGC-1 $\alpha$  shRNA, demonstrating that the effects of these kinases required endogenous PGC-1 $\alpha$ . These data strongly suggest that activation of the PGC-1 $\alpha$  pathway is required for axonal growth rather than being a secondary response to growth.

Nevertheless, we cannot fully exclude the possibility that other pathways are involved. Blocking mitochondrial biogenesis abolished the increase in mitochondrial density; however, a residual increase in neuronal growth remained. Thus, although this indicates that the PGC-1 $\alpha$  pathway is clearly required for the activation of neuronal growth, some other pathways might be marginally involved.

Together, these data suggest that neurons may have a mechanism that senses upcoming energy requirements and that activates the mitochondrial biogenesis machinery prior to the onset of energy deficits.

### The role of energy production in pathologies related to neuronal development

A growing volume of evidence suggests that impaired mitochondrial function may lead to a disruption in normal neural plasticity and reduce cellular resilience (Li et al., 2004; Quiroz et al., 2008; Ruthel and Hollenbeck, 2003; Spillane et al., 2013), which may in turn promote the development or progression of mood and psychotic disorders. Indeed, in many diseases in which mitochondrial defects are present there is high incidence of psychiatric comorbidities. One of the prevailing hypotheses suggests that schizophrenia is a neurodevelopmental disorder that involves the dysfunction of the dopaminergic and glutamatergic system. However, accumulating evidence suggests mitochondria as an additional pathological factor in schizophrenia. Mitochondrial dysfunction and a disturbance in energy metabolism have been observed in schizophrenia patients and, likewise, mitochondrial disorders may present with psychotic, affective and cognitive symptoms (Manji et al., 2012; Robicsek et al., 2013). Recent data revealed that nuclear genes encoding mitochondrially localised proteins are over-represented among large, rare copy-number variations in schizophrenia patients, lending credence to the mitochondrial dysfunction hypothesis (Szatkiewicz et al., 2014). Our results demonstrate that bioenergetics may indeed affect mitochondrial development.

In conclusion, our results suggest that neurons may be capable of signalling for upcoming energy requirements. Growth signals activating CaMKK $\beta$ , LKB1–STRAD or TAK1 pathways also co-activate the AMPK–PGC-1 $\alpha$ –NRF1 axis leading to the generation of new mitochondria (Fig. 8). Earlier activation of mitochondrial biogenesis through these pathways will accelerate the generation of new mitochondria and ensure sufficient energy-producing capability for when other factors for axonal growth are synthesized.

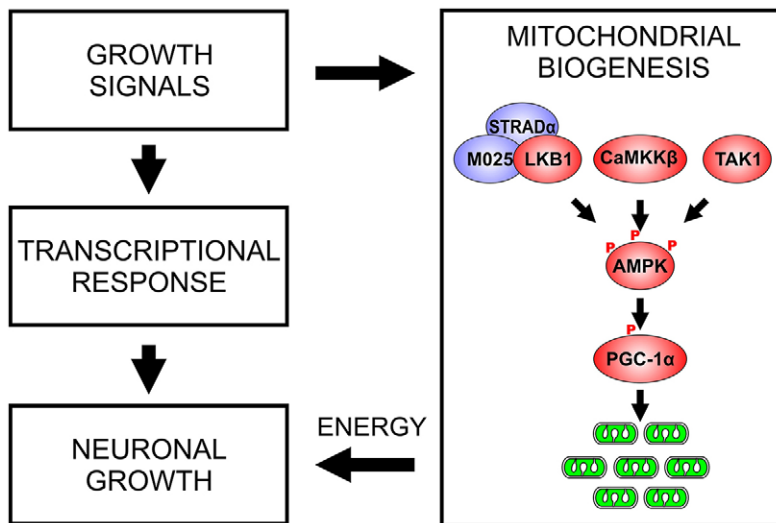


**Fig. 8. Neurons may be capable of signalling for upcoming energy requirements.** Growth signals activating CaMKK $\beta$ , LKB1-STRAD or TAK1 pathways co-activate mitochondrial biogenesis via the AMPK–PGC-1 $\alpha$ –NRF1 axis to generate new mitochondria (green) and the energy required for growth.

## MATERIALS AND METHODS

### Plasmids and chemicals

Plasmids expressing scrambled shRNA or shRNA targeted against rat *PGC-1 $\alpha$*  were obtained from SABiosciences and were previously validated by us (Wareski et al., 2009). Plasmids expressing mitochondrial DsRed2 (mito-DsRed, 632421) and eGFP (6085-1) were from Clontech. The *Renilla* luciferase reporter vector pRL-CMV (E2261) and firefly luciferase reporter pGL4.31[*luc2P*/GAL4UAS/Hygro] vector (C9351) were purchased from Promega. PGC-1 $\alpha$  (10974), GAL4-PGC-1 $\alpha$  with DNA-binding domain (8892), LKB1 (8590), STRAD $\alpha$  (14889), pcDNA3.1\_Lifeact-mCherry (67302), mEos2-Mito-7 (57401), GW1-PercevalHR (49082) and neuron-specific pAAV-hSyn-DsRedExpress (22907) were obtained from Addgene. MO25 (HsCD00331010) was from PlasmID. Plasmids expressing dominant-negative or constitutively active AMPK $\alpha$ 1 and CaMKK $\beta$  isoforms were kind gifts from Dr D. Carling (Imperial College London, UK), NRF1 and dnNRF1 plasmids were from Dr K. Kohno (University of Occupational & Environmental Health, Japan), and TAK1 and dnTAK1 plasmids were from Dr S. Kim (Harvard Medical School, USA). Expression of the transfected plasmids was verified by either western blotting or RT-PCR. AICAR was purchased from Toronto Research Chemicals. TGF $\beta$ 1 (100-21) and TGF $\beta$ 2 (100-35B) were from PeproTech.

### Cell cultures and transfection

Primary cultures of rat cortical cells were prepared from neonatal Wistar rats as described (Wareski et al., 2009). Neurons were grown in Neurobasal A medium supplemented with B27 with or without Phenol Red on poly-L-lysine-coated 96-well white plates, 35-mm plastic or glass-bottom dishes. All culture media and supplements were obtained from Invitrogen.

For transfection of cells growing on glass-bottom dishes, the conditioned medium was replaced with 100  $\mu$ l Opti-MEM I medium containing 2% Lipofectamine 2000 and 1–2  $\mu$ g total DNA containing an equal amount of each plasmid. The dishes were incubated for 3–4 h, after which fresh medium was added. For luciferase analyses, the cells were transfected as described above except that the total volume of the transfection mixture was decreased with proportionally adjusted Lipofectamine and DNA.

### Neuronal maturation, axonal growth and synaptic density

For neuronal maturation experiments, cortical neurons were transfected at day 1 *in vitro* (DIV1) with a plasmid expressing neuron-specific pAAV-hSyn-DsRed Express and plasmids of interest. Live cell morphology was examined visually using a fluorescence microscope (Olympus IX70, 20 $\times$ /0.70 water-immersion objective) on randomly selected fields (minimum 30 fields per dish and three dishes per group) on the indicated days in culture.

Neurons were classified into the four subgroups depending on their maturation stage [classification modified from Dotti et al. (1988)]: I, round cells, formation of lamellipodia; II, immature neuron, sprouting of several minor neurites; III, axon and dendrite formation, neuronal polarisation and branching; IV, neurons with adult-like morphology, ongoing maturation of differentiated processes.

For the analysis of axonal growth, images of cultured cortical neurons (DIV2 to DIV6) were captured using an Olympus IX70 inverted microscope with a 20 $\times$  objective and traced manually using Neurolucida software (MBF Bioscience). The length of the axonal tree, length of the main branch of axon and length of dendrites were measured using Neurolucida Explorer.

To measure live cell dynamics of axonal growth over a period of days, neurons were transfected with GFP-expressing and PGC-1 $\alpha$ -expressing plasmids 4 h after plating onto the compartmented cell culture dish. Transfection medium was exchanged for Phenol Red-free Neurobasal A 3 h later, and cells were further incubated until imaging with a Zeiss LSM 510 META confocal microscope equipped with a Plan-Apochromat 20 $\times$ /0.8 objective. At 8 h after transfection, neurons were placed on the microscope stage housed in a humidified CO $_2$ -enriched atmosphere at 37 $^{\circ}$ C in a climate chamber. Two to three transfected neuronal bodies from each imaging frame were chosen randomly for time-lapse imaging from ten locations per dish compartment. The time interval for sequential image collection was 30 min, and neuronal growth was tracked for 48 h. Image processing and analysis were performed using Zeiss LSM5 Duo version 4.2 software.

### Drug treatment

Effects of inhibition of glycolysis by 2-deoxy-D-glucose or oxidative phosphorylation by sodium azide were assessed as described in the supplementary Materials and Methods.

### Mitochondrial density and length

For whole-cell mitochondrial density measurements, the neurons were transfected with GFP, mito-DsRed, scrambled shRNA or shRNA and plasmids of interest. Four days later, the entire axon and dendrites from randomly selected neurons were visualised using a laser scanning confocal microscope. Neurons were reconstructed using Neurolucida and LSM5 software, and mitochondrial density from at least 20 neurons per group was analysed. For mitochondrial density measurements in axons, ten fluorescence images were captured randomly from each dish using an Olympus IX70 inverted microscope equipped with a WLSM PlanApo 40 $\times$ /0.90 water-immersion objective and an Olympus DP70 CCD camera. Morphometric analysis was performed using MicroImage software (Media Cybernetics). For mitochondrial density (mitochondrial length/axonal length), at least 40 axons per group were analysed (one axon/image). Mitochondrial length measurements were performed as described

previously (Wareski et al., 2009). For estimation of mitochondrial fusion rate and motility, see the supplementary Materials and Methods.

### ATP/ADP ratio measurement

Neuronal endings expressing the ATP/ADP ratio sensor PercevalHR were excited using a 405 nm diode laser and a 488 nm line of an Argon laser and collected using a 494–553 nm emission window. The ratio of fluorescence intensities when exciting at 488 nm divided by 405 nm ( $F_{488nm}/F_{405nm}$ ) was calculated from the collected signal from 50 axonal endings from five dishes per group.

### Luciferase reporter assays

Cortical neurons growing on 96-well plates were transfected at DIV2 as described above using a fusion protein that connected the yeast GAL4 DNA-binding domain with full-length PGC-1 $\alpha$ , an appropriate GAL4-UAS-luciferase reporter and plasmids of interest. All transfections included 0.1  $\mu$ g *Renilla* luciferase (pRL-CMV) plasmid for normalisation. Luciferase assays were performed 3–4 days after transfection using Dual-Glo luciferase assay reagent (Promega) according to the manufacturer's instructions. PGC-1 $\alpha$  activity was determined as relative firefly luciferase luminescence normalised to the *Renilla* luciferase signal, which was measured using a MicroBeta TriLux luminescence counter (PerkinElmer). At least eight independent samples were analysed per group. For details of ATP level estimation by luciferase assay see the supplementary Materials and Methods.

### Expression analysis

Total RNA was isolated on DIV6 from primary neurons using the Qiagen RNeasy Micro Kit. Conversion of 1  $\mu$ g total RNA to cDNA was performed using the SuperScript III RT Kit (Invitrogen). Specific primers were designed for amplification of *PGC-1 $\alpha$*  (*Ppargc1a*), the transcription factors *Nrf1* and *Tfam*, and cytochrome c oxidase subunit genes. qPCR was performed on an ABI PRISM 7900HT Sequence Detection System. Reactions were performed using ABI SYBR Green PCR Master Mix, and raw data were analysed using the  $\Delta\Delta C_t$  method. All genes were normalised to the control gene *Hprt* and cyclophilin A, and values are expressed as fold increases relative to control.

### Statistics

All data are presented as mean $\pm$ s.e.m. The D'Agostino-Pearson omnibus test was used to test the normality of distributions. Comparisons between control and treatment groups were performed by *t*-tests, Mann–Whitney tests or one-way ANOVAs followed by Newman–Keul's post-hoc tests or Kruskal–Wallis tests followed by Dunn's test. Two-way ANOVAs were used to analyse interactions between treatments.  $P < 0.05$  was considered statistically significant.

### Acknowledgements

We thank Dr D. Carling, Dr K. Kohno and Dr S. Kim for providing plasmids; Dr Miriam A. Hickey for valuable comments and linguistic correction; and Ulla Peterson for preparation of primary neurons.

### Competing interests

The authors declare no competing or financial interests.

### Author contributions

A.V. developed the methodology and concepts, performed experiments and analysed the data. M.M., P.W., J.L., M.K., E.A., M.L., V.C. and M.C. performed experiments and analysed the data. A.Z. analysed the data. A.K. developed the concepts, conceived and supervised the study. A.K. and A.V. prepared the manuscript.

### Funding

This work was supported by grants from the Estonian Research Council (Eesti Teadusagentuur) [IUT2-5 and ETF8125]; the European Regional Development Fund [2014-2020.4.01.15-0012]; and from the European Union Horizon 2020 research and innovation programme [under grant agreement 692202].

### Supplementary information

Supplementary information available online at <http://dev.biologists.org/lookup/suppl/doi:10.1242/dev.128926/-DC1>

### References

- Barnes, A. P., Lilley, B. N., Pan, Y. A., Plummer, L. J., Powell, A. W., Raines, A. N., Sanes, J. R. and Polleux, F. (2007). LKB1 and SAD kinases define a pathway required for the polarization of cortical neurons. *Cell* **129**, 549–563.
- Chada, S. R. and Hollenbeck, P. J. (2003). Mitochondrial movement and positioning in axons: the role of growth factor signaling. *J. Exp. Biol.* **206**, 1985–1992.
- Cheng, A., Wan, R., Yang, J.-L., Kamimura, N., Son, T. G., Ouyang, X., Luo, Y., Okun, E. and Mattson, M. P. (2012). Involvement of PGC-1 $\alpha$  in the formation and maintenance of neuronal dendritic spines. *Nat. Commun.* **3**, 1250.
- Dotti, C. G., Sullivan, C. A. and Banker, G. A. (1988). The establishment of polarity by hippocampal neurons in culture. *J. Neurosci.* **8**, 1454–1468.
- Hawley, S. A., Selbert, M. A., Goldstein, E. G., Edelman, A. M., Carling, D. and Hardie, D. G. (1995). 5'-AMP activates the AMP-activated protein kinase cascade, and Ca<sup>2+</sup>/calmodulin activates the calmodulin-dependent protein kinase I cascade, via three independent mechanisms. *J. Biol. Chem.* **270**, 27186–27191.
- Hudmon, A. and Schulman, H. (2002). Structure-function of the multifunctional Ca<sup>2+</sup>/calmodulin-dependent protein kinase II. *Biochem. J.* **364**, 593–611.
- Jäger, S., Handschin, C., St-Pierre, J. and Spiegelman, B. M. (2007). AMP-activated protein kinase (AMPK) action in skeletal muscle via direct phosphorylation of PGC-1 $\alpha$ . *Proc. Natl. Acad. Sci. USA* **104**, 12017–12022.
- Kahn, B. B., Alquier, T., Carling, D. and Hardie, D. G. (2005). AMP-activated protein kinase: ancient energy gauge provides clues to modern understanding of metabolism. *Cell Metab.* **1**, 15–25.
- Lee, C. W. and Peng, H. B. (2008). The function of mitochondria in presynaptic development at the neuromuscular junction. *Mol. Biol. Cell* **19**, 150–158.
- Li, Z., Okamoto, K.-I., Hayashi, Y. and Sheng, M. (2004). The importance of dendritic mitochondria in the morphogenesis and plasticity of spines and synapses. *Cell* **119**, 873–887.
- Manji, H., Kato, T., Di Prospero, N. A., Ness, S., Beal, M. F., Krams, M. and Chen, G. (2012). Impaired mitochondrial function in psychiatric disorders. *Nat. Rev. Neurosci.* **13**, 293–307.
- Mattson, M. P. and Partin, J. (1999). Evidence for mitochondrial control of neuronal polarity. *J. Neurosci. Res.* **56**, 8–20.
- Momicilovic, M., Hong, S.-P. and Carlson, M. (2006). Mammalian TAK1 activates Snf1 protein kinase in yeast and phosphorylates AMP-activated protein kinase in vitro. *J. Biol. Chem.* **281**, 25336–25343.
- Morris, R. L. and Hollenbeck, P. J. (1993). The regulation of bidirectional mitochondrial transport is coordinated with axonal outgrowth. *J. Cell Sci.* **104**, 917–927.
- Prokop, A. (2013). The intricate relationship between microtubules and their associated motor proteins during axon growth and maintenance. *Neural Dev.* **8**, 17.
- Quiroz, J. A., Gray, N. A., Kato, T. and Manji, H. K. (2008). Mitochondrially mediated plasticity in the pathophysiology and treatment of bipolar disorder. *Neuropsychopharmacology* **33**, 2551–2565.
- Robicsek, O., Karay, R., Petit, I., Salzman-Kesner, N., Müller, F.-J., Klein, E., Aberdam, D. and Ben-Shachar, D. (2013). Abnormal neuronal differentiation and mitochondrial dysfunction in hair follicle-derived induced pluripotent stem cells of schizophrenia patients. *Mol. Psychiatry* **18**, 1067–1076.
- Roy Chowdhury, S. K., Smith, D. R., Saleh, A., Schapansky, J., Marquez, A., Gomes, S., Akude, E., Morrow, D., Calcutt, N. A. and Fernyhough, P. (2012). Impaired adenosine monophosphate-activated protein kinase signalling in dorsal root ganglia neurons is linked to mitochondrial dysfunction and peripheral neuropathy in diabetes. *Brain* **135**, 1751–1766.
- Ruthel, G. and Hollenbeck, P. J. (2003). Response of mitochondrial traffic to axon determination and differential branch growth. *J. Neurosci.* **23**, 8618–8624.
- Sakamoto, K., McCarthy, A., Smith, D., Green, K. A., Grahame Hardie, D., Ashworth, A. and Alessi, D. R. (2005). Deficiency of LKB1 in skeletal muscle prevents AMPK activation and glucose uptake during contraction. *EMBO J.* **24**, 1810–1820.
- Shelly, M., Cancedda, L., Heilshorn, S., Sumbre, G. and Poo, M.-M. (2007). LKB1/STRAD promotes axon initiation during neuronal polarization. *Cell* **129**, 565–577.
- Sheng, Z.-H. (2014). Mitochondrial trafficking and anchoring in neurons: new insight and implications. *J. Cell Biol.* **204**, 1087–1098.
- Spillane, M., Ketschek, A., Merianda, T. T., Twiss, J. L. and Gallo, G. (2013). Mitochondria coordinate sites of axon branching through localized intra-axonal protein synthesis. *Cell Rep.* **5**, 1564–1575.
- Szatkiewicz, J. P., O'Dushlaine, C., Chen, G., Chambert, K., Moran, J. L., Neale, B. M., Fromer, M., Ruderfer, D., Akterin, S., Bergen, S. E. et al. (2014). Copy number variation in schizophrenia in Sweden. *Mol. Psychiatry* **19**, 762–773.
- Tantama, M., Martínez-Francois, J. R., Mongeon, R. and Yellen, G. (2013). Imaging energy status in live cells with a fluorescent biosensor of the intracellular ATP-to-ADP ratio. *Nat. Commun.* **4**, 2550.
- Tao, K., Matsuki, N. and Koyama, R. (2014). AMP-activated protein kinase mediates activity-dependent axon branching by recruiting mitochondria to axon. *Dev. Neurobiol.* **74**, 557–573.

- Verstreken, P., Ly, C. V., Venken, K. J. T., Koh, T.-W., Zhou, Y. and Bellen, H. J. (2005). Synaptic mitochondria are critical for mobilization of reserve pool vesicles at *Drosophila* neuromuscular junctions. *Neuron* **47**, 365-378.
- Wareski, P., Vaarmann, A., Choubey, V., Safiulina, D., Liiv, J., Kuum, M. and Kaasik, A. (2009). PGC-1 $\alpha$  and PGC-1 $\beta$  regulate mitochondrial density in neurons. *J. Biol. Chem.* **284**, 21379-21385.
- White, R. E., Yin, F. Q. and Jakeman, L. B. (2008). TGF- $\alpha$  increases astrocyte invasion and promotes axonal growth into the lesion following spinal cord injury in mice. *Exp. Neurol.* **214**, 10-24.
- Woods, A., Johnstone, S. R., Dickerson, K., Leiper, F. C., Fryer, L. G. D., Neumann, D., Schlattner, U., Wallimann, T., Carlson, M. and Carling, D. (2003). LKB1 is the upstream kinase in the AMP-activated protein kinase cascade. *Curr. Biol.* **13**, 2004-2008.
- Woods, A., Dickerson, K., Heath, R., Hong, S.-P., Momcilovic, M., Johnstone, S. R., Carlson, M. and Carling, D. (2005). Ca<sup>2+</sup>/calmodulin-dependent protein kinase kinase- $\beta$  acts upstream of AMP-activated protein kinase in mammalian cells. *Cell Metab.* **2**, 21-33.
- Wu, Z., Puigserver, P., Andersson, U., Zhang, C., Adelmant, G., Mootha, V., Troy, A., Cinti, S., Lowell, B., Scarpulla, R. C. et al. (1999). Mechanisms controlling mitochondrial biogenesis and respiration through the thermogenic coactivator PGC-1. *Cell* **98**, 115-124.
- Xie, M., Zhang, D., Dyck, J. R. B., Li, Y., Zhang, H., Morishima, M., Mann, D. L., Taffet, G. E., Baldini, A., Khoury, D. S. et al. (2006). A pivotal role for endogenous TGF- $\beta$ -activated kinase-1 in the LKB1/AMP-activated protein kinase energy-sensor pathway. *Proc. Natl. Acad. Sci. USA* **103**, 17378-17383.
- Yi, J. J., Barnes, A. P., Hand, R., Polleux, F. and Ehlers, M. D. (2010). TGF- $\beta$  signaling specifies axons during brain development. *Cell* **142**, 144-157.
- Yu, J., Zhang, F., Wang, S., Zhang, Y., Fan, M. and Xu, Z. (2014). TAK1 is activated by TGF- $\beta$  signaling and controls axonal growth during brain development. *J. Mol. Cell Biol.* **6**, 349-351.
- Zong, H., Ren, J. M., Young, L. H., Pypaert, M., Mu, J., Birnbaum, M. J. and Shulman, G. I. (2002). AMP kinase is required for mitochondrial biogenesis in skeletal muscle in response to chronic energy deprivation. *Proc. Natl. Acad. Sci. USA* **99**, 15983-15987.



## **SUPPLEMENTARY MATERIALS AND METHODS**

### **Chemicals**

2-deoxy-D-Glucose (2DG) was purchased from Cayman Europe OU, Estonia. Metformin hydrochloride and sodium azide ( $\text{NaN}_3$ ) were purchased from Toronto Research Chemicals, Canada.

### **Drug treatment**

After 3 days in vitro, culture medium was changed and treatments were initiated. Oxidative ATP production was blocked with  $100 \mu\text{M}$   $\text{NaN}_3$  for 24 hr in the presence of 2.5 mM glucose. 10 mM 2DG was applied to neurons for 24 hr in growth medium in the presence of a reduced amount of glucose (1mM).

### **Mitochondrial fusion rate and motility analysis**

Cortical neuronal cultures were transfected with mito-KikGR1 plasmid and plasmids of interest as described earlier (Cagalinec et al., 2013). A laser scanning confocal microscope (LSM 510 Duo, Carl Zeiss Microscopy GmbH) equipped with a LCI Plan-Neofluar 63 $\times$ /1.3 water immersion DIC M27 objective was used. The temperature was maintained at 37°C using a climate chamber. For fusion analysis, mito-KikGR1 was illuminated with a 488 nm argon laser line to visualize the intense green mitochondrial staining. Selected mitochondria were then photo-converted to red using a 405 nm diode laser and illuminated using a 561 nm DPSS laser. The images were taken at 10s intervals for 10 min, and the fate of all activated mitochondria was followed throughout the time-lapse and the fusion and fission events recorded. The number of fusions and fissions of photo-activated mitochondria was summarised per dish and then averaged over 12 dishes. To compare mitochondrial velocities, 10–20 mitochondria per neurite (including non-activated mitochondria) were tracked and the fraction of time moving and their movement velocity were calculated.

## ATP Levels

Cortical neurons were transfected with plasmids expressing firefly luciferase, *Renilla* luciferase, and the plasmids of interest. To measure firefly luciferase activity, cells were incubated for 10 min with 25µM 1-(4,5-dimethoxy-2-nitrophenyl)ethyl (DMNPE) caged luciferin at 37 °C and the luminescence was measured by MicroBeta® TriLux. To measure *Renilla* luciferase activity, the neurons were lysed and the luminescence was measured using Dual-Glo Luciferase Assay reagent. Firefly luciferase activity from living cells normalized to *Renilla* luciferase activity from lysed cells was used to estimate ATP levels in transfected cells. Sixteen independent samples were analysed per group.

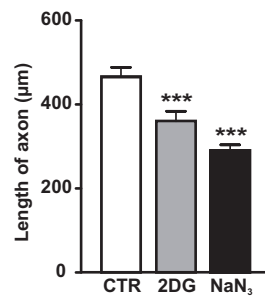


**Fig. S1. Chemical inhibition of glycolysis or oxidative phosphorylation suppresses axonal growth.** On DIV3, oxidative ATP production was blocked with 100  $\mu$ M NaN<sub>3</sub> for 24 hr in the presence of 2.5mM glucose. Glycolytic ATP production was inhibited by applying 10 mM 2DG to neurons for 24 hr in growth medium in the presence of a reduced amount of glucose (1mM). Both treatments significantly reduced axonal growth. \*\*\* $p < 0.001$  compared with the control group (n=40 axons per group).

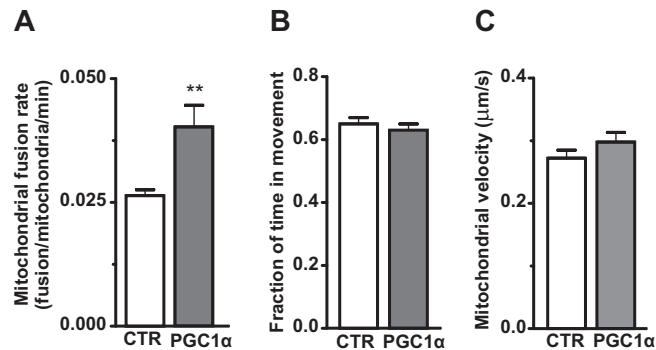


**Fig. S2. Effect of PGC-1 $\alpha$  overexpression on mitochondrial fusion and movement.** Cortical neuronal cultures were co-transfected with mito-KikGR1 and PGC-1 $\alpha$ -overexpressing plasmids and mitochondrial fusion rate and motility parameters were analysed as described in Supplementary Materials and Methods. (A) Mitochondrial fusion rate was significantly increased in PGC-1 $\alpha$ -overexpressing neurons. \*\* $p < 0.001$  compared with the control group,  $n = 12$  dishes. (B and C) The fraction of time spent moving by mitochondria and the average velocity of mitochondria were similar between groups ( $n = 656$  and  $786$  mitochondria in the control and PGC-1 $\alpha$ -overexpressing group respectively,  $p = 0.33$  for fraction of time spent moving and  $p = 0.66$  for mitochondrial velocity).



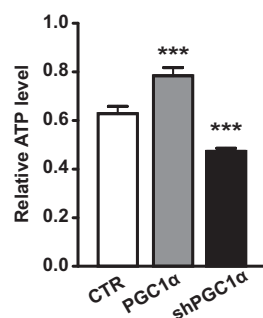


**Fig. S3. The effect of PGC-1 $\alpha$  overexpression or silencing by PGC-1 $\alpha$  shRNA on neuronal ATP levels.** Cortical neurons were co-transfected with firefly- and *Renilla* luciferase-expressing plasmids. Firefly luciferase activity was measured 72 h later in living cells using DMNPE-caged luciferin as a substrate. The results were normalized to *Renilla* luciferase activity measured after cell lysis. \*\*\* $p < 0.001$  compared with the control group (16 independent samples were analysed per group).

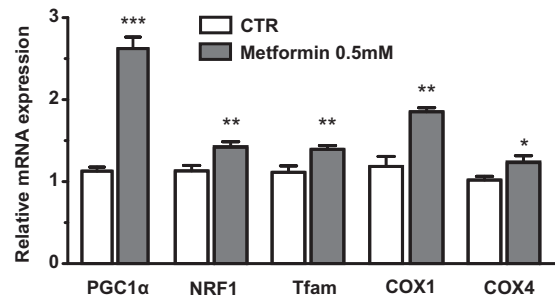


**Fig. S4. Quantitative PCR analysis of mitochondrial biogenesis and energy production-related genes in primary cortical neurons following Metformin treatment.** The mRNA levels of PGC-1 $\alpha$ , NRF1, Tfam, Cox1 and Cox4 (cytochrome c oxidase subunit 1 and 4; encoded in mitochondrial and nuclear DNA, respectively) were normalised to HPRT mRNA levels and expressed relative to control groups (n=4 dishes per group). \*p<0.05, \*\*p<0.01, and \*\*\*p<0.001 compared with respective control groups.